Simultaneous determination of 14 bioactive citrus flavonoids using thin-layer chromatography combined with surface enhanced Raman spectroscopy

Yuzhi Li[a,c], Chengying Zhao[a], Chang Lu[a], Shuaishuai Zhou[a], Guifang Tian[a], Lili He[b], Yuming Bao[a], Marie-Laure Fauconnier[c], Hang Xiao[b,*], Jinkai Zheng[a,*]

[a] Institute of Food Science and Technology, Chinese Academy of Agricultural Sciences, Beijing 100193, China

[b] Department of Food Science, University of Massachusetts, 100 Holdworth Way, Amherst, MA 01003, USA

[c] Laboratory of Chemistry of Natural Molecules, Gembloux Agro-Bio Tech, University of Liege, Gembloux 5030, Belgium

* Corresponding author: Jinkai Zheng, Tel: (086)-010-62819501, Fax: (086)-010-62819501; Hang Xiao, Tel: (413) 545 2281, Fax: (413) 545 1262.

E-mail address: zhengjinkai@caas.cn; hangxiao@foodsci.umass.edu.

Abstract

Citrus flavonoids consist of diverse analogs and possess various health-promoting effects dramatically depending on their chemical structures. Since different flavonoids usually co-exist in real samples, it's necessary to develop rapid and efficient methods for simultaneous determination of multiple flavonoids. Herein, thin layer chromatography combined with surface enhanced Raman spectroscopy (TLC-SERS) was established to simultaneously separate and detect 14 main citrus flavonoids for the first time. These target compounds could be characterized and discriminated when paired with SERS at 6-500 times greater the sensitivity than TLC alone. TLC-SERS exhibited high recovery rates (91.5-121.7%) with relative standard deviation (RSD) lower than 20.8%. Moreover, the established TLC-SERS method was successfully used to simultaneously detect multiple flavonoids in real samples, which exhibited comparable accuracy to high performance liquid chromatography (HPLC) with shorter analytical time (10 *vs* 45 min). All the results demonstrated that this could be a promising method for simultaneous, rapid, sensitive and accurate detection of flavonoids.

Keywords: citrus flavonoids, simultaneous determination, thin layer chromatography, surface-enhanced Raman spectroscopy, HPLC.

Chemical compounds studied in this article

Tangeretin (PubChem CID: 68077); 5-demethyltangeretin (PubChem CID: 96539); nobiletin (PubChem CID: 72344); 5-demethylnobiletin (PubChem CID: 358832); naringenin (PubChem CID: 932); .hesperetin (PubChem CID: 72281); naringin (PubChem CID: 442428); hesperidin (PubChem CID: 10621).

1 Introduction

Flavanones and polymethoxyflavones (PMFs) are the two major flavonoids in citrus fruits, especially in their peels. Citrus flavanones, a class of polyphenolic flavonoids, usually exists as glycoside forms including naringin and hesperidin, which are the most abundant in citrus fruit. They could be converted to their aglycones, namely naringenin and hesperetin (Chen et al., 2018). PMFs, existing exclusively in citrus fruits, are a unique class of flavonoids with two or more methoxyl functional groups (Li, Lo & Ho, 2006). The diversity of PMFs could be contributed to the multiple substituents of the aromatic ring like hydrogen, hydroxyl and methoxyl groups. A number of studies have reported that citrus flavonoids possess various beneficial biological functions such as anticancer (Surichan, Arroo, Ruparelia, Tsatsakis & Androutsopoulos, 2018), anti-inflammatory (Liu, Han, Zhao, Zhao, Tian & Jia), antiatherosclerosis (Kenji, Natsumi, Tai-Ichi & Toshihiko, 2013), antioxidation (Sundaram, Shanthi & Sachdanandam, 2015), anti-viral (Dai et al., 2019), neuroprotection (Chitturi, 2019), among others. Notably, the chemical structures dramatically determine the bioactivities, and different substituents could lead to significant bioactivity variation. For example, hydroxylated PMFs (OH-PMFs), which are formed with hydroxyl groups replacing methoxyl groups or hydrogen of PMFs, exhibit stronger bioactivities than their corresponding parent compounds depending on the structural requirements for optimal active sites (Duan et al., 2017; Li, Hong, Guo, Hui & Ho, 2014; Zheng et al., 2013). However, in most cases, citrus flavonoid analogs exist simultaneously in real samples. It is thus necessary to

develop quick and efficient methods for simultaneous differentiation of citrus flavonoids.

Many methods have been established successfully to analyze citrus flavonoids, such as HPLC-UV (Han, Kim & Lee, 2012; Sayuri, Suwa, Fukuzawa & Kawamitsu, 2011), HPLC-electrochemical detection (ECD) (Li, Pan, Lai, Lo, Slavik & Ho, 2007; Zheng et al., 2015), ultra-performance liquid chromatography (UPLC) (Fayek, 2019; Zhao, 2017), LC-MS (Cho, Su, Sun, Mi & Hong, 2014; Lin, Li, Ho & Lo, 2012), and GC-MS (Stremple, 2015). HPLC-UV was the most widely used method, especially for quantitative analyses, and the limit of detection (LOD) was reported to be as low as 0.02 μg/mL for naringenin (Lin, Hou, Tsai, Wang & Chao, 2014). In our previous study, HPLC-ECD was established as a sensitive and selective technique with lower LOD values of 0.8-3.7 ng/mL OH-PMFs (Zheng et al., 2015). UPLC benefits from a shorter run time than HPLC which can achieve the detection of 16 flavonoids with LODs less than 0.72 μg/mL within 9 min (Zhao, 2017). LC-MS is one of the most common analytical methods with the separation capabilities of HPLC and structural characterization power of mass spectrometry (MS) (Lin et al., 2012; Zheng et al., 2013). It has been used to separate and analyze citrus flavonoids from various matrix with LOD value of 0.02-0.23 μg/mL for six PMFs and six OH-PMFs simultaneously (Lin et al., 2012). Besides, GC-MS is another common analytical method and has been also used for citrus flavonoid analysis (Stremple, 2015). Although the above methods can analyze citrus flavonoids sensitively and effectively, they all have certain limitations.

For instance, HPLC methods are time-consuming, and require complex and rigorous pretreatment; ECD is only effective for compounds with oxidation-reduction property; UPLC is expensive due to the requisite instrument and agents, and difficult to realize on-site detection; MS is also expensive on account of the instrumentation and demanding due to the strict run conditions for the operator; while GC-MS requires a complex derivatization process for citrus flavonoids.

Surface-enhanced Raman spectroscopy (SERS) has been proven to be an efficient analytical tool due to its rapid analytical speed, high sensitivity, signal fingerprinting capabilities, and non-destructive properties (Wen & Lu, 2016). The Raman signals could be significantly enhanced due to an electromagnetic field induced by the surface plasmon resonance and chemical interactions between analyte and substrate (Reguera, Langer, Jimenez & Liz-Marzan, 2017). In the past few years, SERS has been widely used in different fields, such as materials science, various engineering disciplines, medical science, food science and so on (Zheng & He, 2014). Recent studies have also proven the capacity of SERS for the characterization of citrus flavonoids (Ma, Xiao & He, 2016; Zhang et al., 2018; Zheng, Fang, Cao, Xiao & He, 2013). However, it remains difficult to differentiate citrus flavonoid analogs in real samples by virtue of their similar chemical structures, as well as interference of other components in the complex matrix. Thin-layer chromatography (TLC) and high performance TLC (HPTLC) are common separation techniques. Although HPTLC is more stable and accurate than TLC, and has been reported as an ideal method for fingerprinting studies of plant samples

(Meier & Spriano, 2010; Mikropoulou, Petrakis, Argyropoulou, Mitakou, Halabalaki & Skaltsounis, 2019; Oellig, Schunck & Schwack, 2018), TLC is more commonly used with several notable advantages, such as low cost and simplicity. However, TLC is limited in its use for quantitative analysis due to relatively low accuracy. The combination of TLC and SERS allows separation and subsequent spectral detection of chemical species from complex matrices, and multiple successful examples of its use have been reported (Germinario, Garrappa, Dambrosio, Werf & Sabbatini, 2018; Zhu, Chen, Han, Yuan & Lu, 2017).

In this study, TLC-SERS was developed to achieve simultaneous, sensitive and accurate detection of 14 citrus flavonoids (**Fig. 1A**) for the first time. In order to obtain better separation and detection efficiency, two-dimensional (2D) TLC was carried out. The chromatographic elution profile of 14 citrus flavonoids on TLC and characteristic signatures of SERS spectra were also systematically studied. This study has the potential to further advance the rapid and efficient determination of different flavonoids in the citrus industry, as well as other applications for functional foods.

2 Materials and methods

2.1 Reagents and chemicals

Vanillin, concentrated sulfuric acid (18.4 M), acetic acid, ethanol, petroleum ether (PE), acetone (AT), dichloromethane (DCM), methanol (MT), ferric chloride ($FeCl_3$), and hydrochloric acid (11.7 M) were of analytical grade and purchased from Sinopharm Chemical Reagent Co., Ltd (Beijing, China). Acetonitrile (ACN), tetrahydrofuran (THF)

and trifluoroacetic acid (TFA) were of HPLC grade bought from Fisher Scientific. Normal phase TLC plates (250 μm layer) were bought from Merk kGaA (Darmstadt, Germany). Silver nitrate (99%) and zinc (99%) were bought from Eastern Chemical Works (Shanghai, China). Silver (Ag) dendrites were prepared through a displacement reaction involving zinc and silver nitrate according to our previously published method (He et al., 2013). Tangeretin (**1**) and nobiletin (**3**) were purchased from Quality Phytochemicals LLC (Edison, NJ, USA). 5-demethyltangeretin (**2**), 3′-demethylnobiletin (**4**), 4′-demethylnobiletin (**5**), 3′,4′-didemethylnobiletin (**6**), 5-demethylnobiletin (**7**), 5,3′-didemethylnobiletin (**8**), 5,4′-didemethylnobiletin (**9**) and 5,3′,4′-tridemethylnobiletin (**10**), were obtained by multi-steps synthesis we have reported before (Lin et al., 2012; Zheng et al., 2015). Naringenin (**11**), hesperetin (**12**), naringin (**13**) and hesperidin (**14**) were purchased from ACROS Organics (New Jersey, USA). All their purities were up to 98% (HPLC), and their chemical structures have been elucidated by MS and NMR spectra (Zheng et al., 2013). Ultrapure water was further purified from deionized water using a Milli-Q system (Millipore, Bedford, USA).

2.2 TLC separation of 14 citrus flavonoid analogs

Compounds **1-12** were dissolved in methanol to 5 mM, and gradient-diluted to 2.5, 1.0, 0.5, 0.1, and 0.05 mM were used for LOD determination on the TLC plate. Meanwhile, compounds **13** and **14** were prepared in a series of concentration at 1, 0.5, 0.1, 0.05, and 0.01 mM. Two rapid in-situ visualization methods were applied here. The

first utilized UV fluorescence at excitation wavelengths of 254 nm and 365 nm. The second utilized two different TLC visualization reagents. The general visualization reagent contained 1% vanillin in ethanol with several drops of concentrated sulfuric acid. The special visualization reagent for compounds with a phenolic hydroxyl group was prepared with 3% $FeCl_3$ dissolved in 0.5 M hydrochloric acid solution. Various elution systems (DCM: MT= 10: 1, 15: 1, 20: 1, 30: 1 and 50: 1; PE: AT= 8: 2, 7: 3, 6: 4, 5: 5, and 4: 6) were conducted. The elution systems of DCM: MT= 20: 1 and PE: AT= 6: 4 performed relatively high separation efficiency for 14 compounds in 1D TLC separation. In order to achieve efficient separation, 2D TLC analysis through two elution systems (DCM: MT at 20: 1 and PE: AT at 6: 4) was carried out. 1% acetic acid in solution was produced in the DCM: MT system to improve the diffused zone shape. 2 μL of the mixture was loaded onto the bottom-right of thin liquid chromatography plates (8×8 cm^2) and eluted with DCM: MT= 20: 1 containing 1% acetic acid, then rotated to the right and eluted with PE: AT= 6: 4. The time for 2D TLC separation was about 5 min. The retention factor (R_f) value was calculated by measuring the location of each spot (dc, distance from the origin of the plate to the center of the eluted spot) and the distance from the origin to the solvent front (ds). The R_f value was calculated from the dc/ds ratio. The color and LOD value for each sample were also recorded.

2.3 SERS detection after TLC separation

After 2D TLC separation, each spot of a citrus flavonoid from the final TLC plate was stripped and put into microcentrifuge tubes with 100 μL methanol. After

centrifugation (3000 rpm, 2 min), the supernatant was evaporated under vacuum and dissolved in 10 μL methanol in preparation for detection. The time for these procedures was about 3 min. Meanwhile, the substrate method for SERS analysis reported in our previous study was used here (Ma et al., 2016). In brief, 5 μL of Ag dendrites were deposited onto a glass slide first and air-dried. Then, 2 μL of test sample solution was deposited on the dried Ag for Raman measurement after drying. SERS detection was performed on a DXR Raman microscope (HORIBA), facilitated with a 514 nm excitation laser and a 50× objective confocal microscope (2 μm spot diameter and 5 cm^{-1} spectral resolution). The measured condition for each sample was as follows: 3 mW of laser power, 50 μm slit width for 10 s integration time. Five spots were chosen randomly for each sample. SERS spectra were collected and analyzed through LabSpec Application software and TQ Analyst software (v8.0, Thermo Fisher Scientific), respectively. Data pre-processing algorithms through second-derivative transformation and smoothing were employed to remove the baseline shift, reduce spectral noise, and separate overlapping bands. Discriminant analysis of the SERS spectra was determined by principal component analysis (PCA), obtained according to Ward's algorithm within 1100-1800 cm^{-1}. Partial least-squares (PLS) analysis was used to quantitative analysis to predict the sample amount.

2.4 Validation of the TLC-SERS method

The PLS model was evaluated by correlation coefficient (R), root-mean-square error of calibration (RMSEC), and the root-mean-square error of prediction (RMSEP). The

linear ranges were determined when R was above 0.9544, with different samples of various concentrations distributed between 30–350 μM. The limit of quantitation (LOQ) value was determined as the lowest concentration among the linear range, with the ratio of 10: 3 to limit of detection (LOD) value. Recovery rates of the extraction and detection method were obtained by analyzing known amounts of standard flavonoids (50 and 100 μM, respectively). Precision of detection was determined from the three batches at 50 and 100 μM flavonoid concentration, and expressed as RSD (%, relative standard deviations).

2.5 HPLC-UV analysis of 14 citrus flavonoids

All the 14 compounds were dissolved in methanol at a final concentration of 1 mM for the following HPLC analysis. The Ultimate 3000 Series HPLC system (Thermo Scientific, USA) consisted of a double ternary gradient pump (DGP-3600), and an auto-sampler (WPS-3000 SL/TSL). Instrument control and data processing were performed with Chromeleon® 7. Ascentis RP-Amide reversed-phase HPLC column (15 cm×4.6 mm id, 3 μm) (Sigma-Aldrich, MO, USA) using gradient elution with the mobile phase A: 75% water, 20% ACN and 5% THF; the mobile phase B: 50% water, 40% ACN and 10% THF (pH values of both mobile phases were adjusted to 3.00 using TFA) (Zheng et al., 2015). The optimal elution gradient program was as follows: 0-5.0 min, 10-50% B; 5.0-35.0 min, 50% B; 35.0-40.0 min, 100% B; and 40.0-45.0 min, 10% B followed by a 5 min equilibrium time using the initial gradient between individual runs with 1 mL/min flow rate and 10 μL injection volume (Zheng et al., 2015). An equimolar

mixture of all 14 compounds at 50 μM was used for HPLC analysis. The UV-vis scanning for these compounds were set from 190-500 nm using DAD detector. The wavelength range was divided artificially into two parts, including band I (300-400 nm) and band II (220-280 nm), caused by the cross-conjugate system with cinnamoyl group and benzoyl group, respectively. Indeed, 280 nm and 330 nm are characteristic absorbance wavelength for flavonoids. Here, calibration curves were constructed with serial dilutions (0.1, 0.5, 1, 5, 10, 20, 40, 80 and 160 μM) for each component in the test solutions under 280 nm for compounds **1**-**14**.

2.6 Real sample preparation and detection using TLC-SERS and HPLC-UV

Three real samples (orange juice, fresh orange peel, and mice fecal sample fed with compound **7**) were prepared for TLC-SERS and HPLC-UV analysis. For the fresh orange juice sample (sample 1), 1 mL of Gannan navel orange juice was taken for later flavonoids extraction. An equivalent volume of methanol was added to dissolve and extract flavonoids under ultrasonic bath (80 Hz, 10 min) for three times and combined. After centrifugation (3000 rpm, 5 min), the supernatant was dried under vacuum, and finally dissolved in 100 μL of methanol for further analysis. Using the same extraction process, 1 g of orange peel (sample 2) and fecal sample from CF-1 male mice fed with nobiletin supplementation (500 ppm) for 1 week (sample 3) were also used for flavonoids extraction, which were finally dissolved in 100 μL methanol for further analysis. For TLC-SERS analysis, the components of flavonoids contained in each sample were analyzed by R_f value and SERS characteristic peaks, and the content was

calculated according to the standard curve in PLS analysis. For HPLC-UV analysis, the qualitative and quantitative analysis were carried out based on the retention time, UV-vis spectroscopy, and standard curve. The detection ability of TLC-SERS for flavonoids in real samples was evaluated by comparing accuracy, standard variance, and detection time with HPLC-UV.

2.7 Data analysis

All analyses for SERS and HPLC were performed in triplicate at least, and the results were presented as means ± standard deviation of three independent experiments.

3 Results and discussion

3.1 TLC separation and analysis of 14 citrus flavonoids

3.1.1 Separation of citrus flavonoids on normal-phase TLC plate

Were simultaneously separated 14 citrus flavonoids (**Fig. 1A**) on normal-phase TLC plates, various elution systems were conducted initially as a screen. As a result, the systems of DCM: MT at 20: 1 and PE: AT at 6: 4 were chosen as the optimal conditions with relatively high separation efficiency. 1% acetic acid was produced in the DCM/MT system to eliminate a slight observed tailing effect. Under this condition, the R_f values of these citrus flavonoids were from 0 to 0.97 with the sequence as following: **2** (0.97) ≈ **7** (0.95) > **1** (0.77) ≈ **9** (0.77) > **8** (0.74) ≈ **3** (0.73) > **12** (0.70) ≈ **4** (0.69) ≈ **5** (0.68) > **11** (0.48) > **10** (0.45) > **6** (0.38) > **13** (0) ≈ **14** (0) (**Table 1**). The R_f values could reflect the polarity of the compounds to a large extent, from which it could be speculated that more hydroxyl functional groups present on the B ring, the more polar

it is relatively (**6** *vs* **4** *vs* **3**, **10** *vs* **8** *vs* **7**, **5** *vs* **3**, and **9** *vs* **7**) (Wojtanowski & Mroczek, 2018; Hvattum & Ekeberg, 2003). Interestingly, the demethylation of the 5′ position methoxyl made the compound more hydrophobic which might be due to the formation of an intra-molecular hydrogen bond between the hydroxyl and the adjacent 4-ketone carbonyl groups (**2** *vs* **1**, **7** *vs* **3**, **8** *vs* **4**, **9** *vs* **5**, and **10** *vs* **6**) (Wojtanowski & Mroczek, 2018). Although some could be separated significantly, compounds **2** and **7**, **3** and **8**, **1** and **9**, as well as compounds **4**, **5**, and **12** could not be separated from each other efficiently (**Fig. 1B**). Since the R_f value may vary in different elution systems, another system composed of mixed aprotic solvents was also tested to achieve better separation. Improved separation of compounds **2** (0.62) and **7** (0.57), **1** (0.53) and **9** (0.51), **3** (0.46) and **8** (0.48), and **4** (0.36), **5** (0.38), and **12** (0.42) was achieved with the elution using PE: AT= 6: 4 (**Fig. 1C**). However, it was still not efficient enough. Therefore, 2D-TLC with the two elution systems above was further carried out. As a result, all compounds, except compounds **13** and **14** could be separated efficiently and differentiated, demonstrating the high efficiency of the 2D-TLC separation for simultaneous separation of multiple citrus flavonoids (**Fig. 1D**).

3.1.2 Visualization and LOD values of citrus flavonoids on TLC plate

UV fluorescence (254 nm and 365 nm) and visual staining (vanillin-H_2SO_4 and $FeCl_3$-HCl) were used here. All showed similar UV fluorescence response under 254 and 365 nm due to their shared flavonoid skeletal structure. As shown in **Table 1**, all of the compounds exhibited the same inactivity under excitation at 254 nm, shown as a

dark spot. Under 365 nm excitation, flavonoids with C5-OMe on the A ring (compounds **1**, **3**, **4**, **5**, and **6**) and flavanone aglycones (compounds **13** and **14**) reacted as a bright spot, while the other flavonoids (compounds **2**, **7**, **8**, **9**, **10**, **11** and **12**) exhibited no activity at the emissions screened as a dark spot. The LOD of the 14 compounds under 254 nm fluorescence ranged from 0.5 to 2.5 mM, while 0.1 to 2.5 mM under 365 nm. For visual staining, all the PMFs and OH-PMFs exhibited yellow color, while flavanones cannot be detected by vanillin-H_2SO_4 stain. These results demonstrated the necessity of CH=CH at C2 for differentiation. As shown in **Table 1**, only flavonoids with hydroxyl groups could be detected by $FeCl_3$ visual staining, and the color was in proportion to the number and position of hydroxyl groups in the polyphenol. Flavones with C5-OH exhibited darker color (compounds **2**, **7**-**10** *vs* **4**-**6**), which indicated that the hydroxyl group at C5 site plays a major role in $FeCl_3$ visual staining. It might be attributed to the stronger reducing ability of hydroxyl group at C5 site. Compounds **13** and **14** had a lower LOD value (1 mM) under $FeCl_3$ visual staining compared to other compounds (5 mM), which might be due to the presence of more hydroxyl groups. All the features could be used to identify and differentiate different citrus flavonoids.

3.2 SERS qualitative and quantitative detection after TLC separation

3.2.1 Qualitative detection of citrus flavonoids by TLC-SERS

Second-derivative transformation was applied to average raw SERS spectra (N= 5) to separate overlapping bands and remove baseline shifts, which makes characteristic

peaks in SERS spectra easily recognizable (**Fig. 2A**) (Ma et al., 2016; Zhang et al., 2018; Zheng et al., 2013). In general, most of the citrus flavonoids showed similar spectra below 1000 cm^{-1} owing to the similar skeletal structure. The characteristic peaks were mainly at 1550-1650 cm^{-1} (assigned to C=O stretch) and 1100-1500 cm^{-1} (assigned to different O-H bend) (**Table S1**) (Huang & Chen, 2018; Sanchez-Cortes & Garcia-Ramos, 2000; Zaffino, Bedini, Mazzola, Guglielmi & Bruni, 2016). In accordance with chemical structures, the 14 flavonoids could be divided into four categories as tangeretin analogs (compounds **1** and **2**), nobiletin analogs (compounds **3**-**6**), 5-demethylnobiletin analogs (compounds **7**-**10**), and flavanone analogs (compounds **11**-**14**) through SERS spectra. The bands at 1650-1700 cm^{-1}, contributed from C(H)-C(H), could significantly distinguish the flavanones from the other three analogs. The flavonoids with two substituent groups on their B ring possessed marked bands at 1330-1430 cm^{-1}, which belonged to OH bend (ip), C3′-OH and C4′-OH bend (ip), and could differentiate nobiletin and 5-demethylnobiletin analogs from tangeretin analogs. For tangeretin analogs, the 1542 cm^{-1} peak was mainly from the C=O stretch in combination with ring quinoidal stretches of compound **1**, with a 1577 cm^{-1} peak for compound **2**. The peaks of C-H bend could also be used to distinguish compounds **1** (1458 cm^{-1}) and **2** (1443 and 1537 cm^{-1}). Nobiletin analogs with a methoxyl group on C5 had SERS bands at 1330-1350 cm^{-1} corresponded to the C-H bend (ip), and it could be obviously distinguished from 5-demethylnobiletin analogs through bands at 1350-1375 cm^{-1} of OH bend (ip) C5 hydroxyl, as well as 1130-1150 cm^{-1} of 5-OH bend. The

appearance of bands at 1400-1450 cm^{-1} of C3′-OH and C4′-OH bend (ip) could be considered as the characteristic peaks for each compound. For flavanone analogs, the band at 1221 cm^{-1} belonged to *ν*(C-H) of CH_3 could be used to distinguish hesperetin analogs (compounds **12** and **14**) from naringenin analogs (compounds **11** and **13**). However, using SERS alone, it is difficult to differentiate glucosides and the corresponding aglycones such as compounds **11**/**13** and **12**/**14**, respectively. Due to the working separation of TLC, an efficient detection was possible for all compounds except **11**/**13** and **12**/**14** with the combination of TLC and SERS. PCA was further used to verify the discrimination ability of SERS. The four kinds of analogs (tangeretin, nobiletin, 5-demethylnobiletin, and flavanone analogs) clustered together (**Fig. 2B**). The PCA results demonstrated that the potential capacity of SERS to distinguish different citrus flavonoids even those of similar chemical structure.

3.2.2 Quantitative analysis of citrus flavonoids by TLC-SERS

During the quantitative analysis, the SERS signal intensity was observed to increase along with the concentration from 30 to 350 μM. The peaks at 1604, 1636, 1553, 1559, 1555, 1546, 1631, 1620, 1629, 1609, 1126, 1550, 1131 and 1546 cm^{-1} were chosen for LOQ and PLS analysis of compounds **1**-**14**, respectively. As shown in **Table 2**, the LOQ values for compounds **1**-**4** and **8** were 50 μM, which were slightly higher than the other compounds (30 μM). Based on these, the LOD could be determined as about 16.7 μM for compounds **1**-**4** and **8**, and 10 μM for the others, which were 6-500 times lower than those determined by TLC visualization. The quantification ability of the method

was further investigated by PLS. The relationship between the predicted concentration and actual concentration with R, RMSEC and RMSEP was found to be 0.9544-0.9962, 5.5-32.8 and 12.9-39.6, respectively. The relatively low value for RMSEC and RMSEP, and high value for R (close to 1), demonstrated the reliability of SERS for quantitative analysis using the PLS calibration curve based on the characteristic peaks (**Fig. 2C**). In short, TLC-SERS detection had lower LOD values for flavonoids than other normal TLC visualization methods. At the same time, fingerprinting was used prior to TLC for qualitative analysis. With the combination of TLC and SERS, simultaneous separation and detection of all the 14 citrus flavonoid analogs could be achieved. For TLC-SERS method, recovery rates of the extraction and detection method ranged from 91.5 to 121.7 with RSD ≤ 20.8 for all 14 flavonoids at 50 and 100 μM (**Table 2**), indicating that influences from extraction to quantitation was unneglectable, but still acceptable. The precision was expressed as RSD between 1.5% and 11.8%, which demonstrated the good reproducibility of the method established in this study. Additionally, TLC-SERS showed the potential to be a rapid and efficient method for analysis of citrus flavone analogs from complex matrices based on the efficient separation of TLC and the high sensitivity of SERS.

3.3 HPLC-UV analysis of 14 citrus flavonoids

3.3.1 HPLC separation of citrus flavonoids

HPLC has been considered as the golden standard analytical method for a wide array of chemical compounds. In order to evaluate the established TLC-SERS method, 14

citrus flavonoids were ran simultaneously on HPLC. As a result, all the compounds could be separated under the tested elution gradient profile except for compounds **1** and **11** (**Fig. 3A**). Similar to R_f value, the retention time could also be used to speculate the polarity of the 14 compounds. As one would expect, substituent groups including the group type (hydroxyl or methoxyl group) and position (5-, 3′-, and/or 4′-position) had an observed effect on the retention time. In general, demethylation increased the polarity, and 3′-demethylation was more effective than 4′-demethylation (compounds **4**/**5** and **8**/**9**). In addition, compounds became more polar after C3′-H substitution by -OMe (compounds **1**/**3**). However, demethylation at C5 caused an obvious decrease of the polarity, which might be due to the formation of an intra-molecular hydrogen bond between hydroxyl and the adjacent 4-ketone carbonyl (**2** *vs* **1**, **7** *vs* **3**, **8** *vs* **4**, **9** *vs* **5**, and **10** *vs* **6**). The results were roughly consistent with TLC analysis, despite that the polarity sequence of a few compounds were not coincident with each other. This might due to the different absorption capacity between compounds and chromatographic matrix (Eric, 2008). Quantitative analysis was also carried out via absorption at 280 nm. As shown in **Table S2**, all the 14 citrus flavonoids had good linear relationships in the range of 5-160 μM with R values higher than 0.9995. The LOD values were 1.5 μM for compounds **7** and **10**, and 0.3 μM for others, indicating higher sensitivity of HPLC for the 14 flavonoids in contrast with TLC-SERS. Although various elution systems were attempted, compounds **1** and **11** still could not be separated simultaneously.

3.3.2 UV adsorption of 14 citrus flavonoids

The UV adsorption spectra from 190 nm to 500 nm were also investigated to differentiate 14 citrus flavonoids (**Fig. 3E**). They could be divided artificially into two parts: band I (300-400 nm) and band II (220-280 nm), which were caused by the cross-conjugate system with the cinnamoyl group and benzoyl group, respectively. Generally, both band I and II were exhibited in PMFs and OH-PMFs UV spectra, while only band II was present for flavanones due to the lack of conjugation of cinnamoyl. In detail, the higher the degree of oxygen substitution on ring B, the higher the red shift of band I (**1, 2** *vs* **3**-**10**). Substituents of -OH/-OMe made the band I red-shift which might due to the p-π conjugation between the substituents and benzoyl. Furthermore, the electron-donating effect of -OH was stronger than -OMe, as a result, red shift was also caused by demethylation (**4** *vs* **5** *vs* **6**, and **7** *vs* **8** *vs* **9**). However, the effects of demethylation positions on the red-shift phenomena were different. Demethylation at C5 made band I red shift the most, followed by 4′-demethylation, and then 3′-demethylation. As for band II, 5-demethylation led to red shift while demethylation at 3′- and 4′- position led to blue shift. Moreover, the band II changed from a single peak to cross peak if there were two or more oxygen substitutions on ring B (**1, 2** *vs* **3**-**10**). For flavanone analogs, band I disappeared due to the lack of cinnamoyl conjugation system. Thus, band II was used as characteristic absorption band for PMFs UV analysis. Although the UV absorption features differs from each other depending on the chemical structures, it is difficult to be used for the identification of different compounds without standards. In

this respect, TLC-SERS might be preferred for the simultaneous analysis of flavonoids in real samples.

3.4 Determination of citrus flavonoids in real samples

Three real samples which might contain multiple citrus flavonoids were used here to further evaluate the efficiency of the established TLC-SERS method. For orange juice sample, the extracts were analyzed with 2D TLC according to the above conditions, and three main spots were screened on TLC plates with similar R_f values to compounds **1**, **3**, **13**/**14** respectively. Then, the separated compounds were subjected to further qualitative and quantitative analyses based on the SERS characteristic peaks and PLS calibration curves. They were confirmed to be compounds **1**, **3**, **13** and **14** with the contents of 3.9, 46.0, 87.8 and 169.4 μg/mL, respectively (**Table 3**), which were consistent with a previous report for dried citrus peel extraction research (Zhang et al., 2019). Similarly, compounds **1**, **3**, **13** and **14** were also detected in the orange peel sample (sample 2) with the contents of 43.2, 212.5, 467.1 and 986.5 μg/g, respectively. For sample 3, depending on the R_f value, four compounds were recognized and determined to be compounds **7**-**10**—the *in vivo* metabolites of 5-demethylnobiletin (Zheng et al., 2013). The "fingerprint" information from SERS spectra further confirmed the four components with the concentrations of 34.6, 3.7, 11.1, and 29.3 ng/g, respectively. The citrus flavonoids contained in the three samples were also analyzed through HPLC-UV. As shown in **Table 3**, the results were consistent with TLC-SERS with a deviation within 2.4% and 25.9%, which indicated that the detection efficiency

of the established TLC-SERS method for citrus flavonoids was comparable to a "gold-standard" analytical method, HPLC-UV. Considering that the total analytical time for TLC-SERS was only about 10 minutes (5 min for TLC separation, 3 min for sample recovery after TLC separation, and 2 min for SERS detection), but up to 45 minutes for HPLC analysis, the TLC-SERS method established here could be a preferred method for rapid, sensitive, and efficient simultaneous detection of citrus flavonoids or other functional components from complex samples. This method could be applied for the rapid, sensitive and efficient simultaneous detection of citrus flavonoids even other components from real samples, for example functional components from fruits and vegetables, the content and yield of functional components during extraction or processing, and metabolites and health markers in biological experiments and so on.

4 Conclusion

In summary, TLC-SERS was established for simultaneous detection of 14 citrus flavonoids for the first time. It was proven that 2D TLC eluted with DCM: MT at 20: 1 and PE: AT at 6: 4, could achieve efficient separation for most, if not all, of the target compounds. SERS with "fingerprint" properties was further used to differentiate and identify each compound after TLC separation. As a result, TLC-SERS was successfully established to characterize and distinguish all the 14 citrus flavonoids with similar chemical structures and physicochemical properties, which exhibited significantly higher sensitivity (LOD values 10.0-16.7 μM) than TLC analysis (LOD values 0.1-5.0 mM). More importantly, the detection efficiency for citrus flavonoids from real samples

was comparable to HPLC with low deviation (2.4-25.9%). Along with short analytical time, the TLC-SERS method established here could be a promising method to achieve simultaneous, sensitive and accurate detection of flavonoids in real samples. It would further advance the rapid and efficient determination of different flavonoids in citrus industry, as well as other applications in functional foods.

Conflicts of interest

The authors declare no competing financial interest.

Acknowledgements

The authors would like to acknowledge the financial support provided by National Natural Science Foundation of China (Nos. 31428017). We also appreciate the financial support from Agricultural Science Innovation Program (S2019XK02) and Elite Youth Program of Chinese Academy of Agricultural Sciences.

Supporting information

HPLC-UV quantitative results of 14 citrus flavonoids and their corresponding modes of 14 citrus flavonoids on SERS spectra.

References

Chen, T., Su, W., Yan, Z., Wu, H., Zeng, X., Peng, W., Gan, L., Zhang, Y., & Yao, H. (2018). Identification of naringin metabolites mediated by human intestinal microbes with stable isotope-labeling method and UFLC-Q-TOF-MS/MS. *Journal of Pharmaceutical and Biomedical Analysis, 161*, 262−272. https://doi.org/10.1016/j.jpba.2018.08.039.

Chitturi, J. S., & Kannurpatti, S. (2019). Beneficial effects of kaempferol after developmental traumatic brain injury is through protection of mitochondrial function, oxidative metabolism, and neural viability. *Journal of Neurotrauma, 36*, 1264−1278. https://doi.org/10.1089/neu.2018.6100.

Cho, H. E., Su, Y. A., Sun, C. K., Mi, H. W., & Hong, J. T. (2014). Determination of flavonoid glycosides, polymethoxyflavones, and coumarins in herbal drugs of citrus and poncirus fruits by high performance liquid chromatography–electrospray ionization/tandem mass spectrometry. *Analytical Letters, 47*, 1299−1323. https://doi.org/10.1080/00032719.2013.871548.

Dai, W., Bi, J., Li, F., Wang, S., Huang, X., Meng, X., Sun, B., Wang, D., Kong, W., Jiang, C., & Su W. (2019) Antiviral efficacy of flavonoids against Enterovirus 71 infection in vitro and in newborn mice. *Viruses*, 11, 625−638. https://doi.org/10.3390/v11070625.

Duan, L., Dou, L. L., Yu, K. Y., Guo, L., Baizhong, C., Li, P., & Liu, E. H. (2017). Polymethoxyflavones in peel of Citrus reticulata 'Chachi' and their biological

activities. *Food Chemistry, 234*, 254−261. https://doi.org/10.1016/j.foodchem.2017.05.018.

Eric, L. (2008). Overview of the retention in subcritical fluid chromatography with varied polarity stationary phases. *Journal of Separation Science, 31*, 1238−1251. https://doi.org/10.1002/jssc.200800057.

Fayek, N. M. F., M. A., Abdel, A. R., Moussa, M. Y., Abd-Elwahab, S. M., & Tanbouly, N. D. (2019). Comparative metabolite profiling of four citrus peel cultivars via ultra-performance liquid chromatography coupled with quadrupole-time-of-flight-mass spectrometry and multivariate data analyses. *Journal of Chromatographic Science, 57*, 349−360. https://doi.org/10.1093/chromsci/bmz006.

Germinario, G., Garrappa, S., Dambrosio, V., Werf, I. D. V. D., & Sabbatini, L. (2018). Chemical composition of felt-tip pen inks. *Analytical and Bioanalytical Chemistry, 410*, 1079−1094. https://doi.org/10.1007/s00216-017-0687-x.

Han, S., Kim, H. M., & Lee, S. (2012). Simultaneous determination of polymethoxyflavones in Citrus species, Kiyomi tangor and Satsuma mandarin, by high performance liquid chromatography. *Food Chemistry, 134*, 1220−1224. https://doi.org/10.1016/j.foodchem.2012.02.187.

Huang, C. C., & Chen, W. (2018). A SERS method with attomolar sensitivity: a case study with the flavonoid catechin. *Mikrochimica Acta, 185*, 120−128. https://doi.org/10.1007/s00604-017-2662-9.

Hvattum, E., & Ekeberg, D. (2003). Study of the collision-induced radical cleavage of

494 flavonoid glycosides using negative electrospray ionization tandem quadru-pole
495 mass spectrometry. *Journal of Mass Spectrometry, 38*, 43−49.
496 https://doi.org/10.1002/jms.398.
497 Kenji, O., Natsumi, H., Tai-Ichi, S., & Toshihiko, H. (2013). Polymethoxyflavonoids
498 tangeretin and nobiletin increase glucose uptake in murine adipocytes.
499 *Phytotherapy Research, 27*, 312−316. https://doi.org/10.1002/ptr.4730.
500 Li, S., Hong, W., Guo, L., Hui, Z., & Ho, C. T. (2014). Chemistry and bioactivity of
501 nobiletin and its metabolites. *Journal of Functional Foods, 6*, 2−10.
502 https://doi.org/10.1016/j.jff.2013.12.011.
503 Li, S., Lo, C. Y., & Ho, C. T. (2006). Hydroxylated polymethoxyflavones and
504 methylated flavonoids in sweet orange (*Citrus sinensis*) peel. *Journal of*
505 *Agricultural & Food Chemistry, 54*, 4176−4185. https://doi.org/10.1021/jf060234n.
506 Li, S., Pan, M. H., Lai, C. S., Lo, C. Y., Slavik, D., & Ho, C. T. (2007). Isolation and
507 syntheses of polymethoxyflavones and hydroxylated polymethoxyflavones as
508 inhibitors of HL-60 cell lines. *Bioorganic and Medicinal Chemistry, 15*,
509 3381−3389. https://doi.org/10.1016/j.bmc.2007.03.021.
510 Lin, S. P., Hou, Y. C., Tsai, S. Y., Wang, M. J., & Chao, P. D. L. (2014). Tissue
511 distribution of naringenin conjugated metabolites following repeated dosing of
512 naringin to rats. *BioMedicine, 4*, 1−6. https://doi.org/10.7603/s40681-014-0016-z.
513 Lin, Y. S., Li, S., Ho, C. T., & Lo, C. Y. (2012). Simultaneous analysis of six
514 polymethoxyflavones and six 5-hydroxy-polymethoxyflavones by high

515 performance liquid chromatography combined with linear ion trap mass
516 spectrometry. *Journal of Agricultural & Food Chemistry, 60*, 12082−12087.
517 https://doi.org/10.1021/jf303896q.
518 Liu, Z., Han, Y., Zhao, F., Zhao, Z., Tian, J., & Jia, K. (2019). Nobiletin suppresses
519 high-glucose-induced inflammation and ECM accumulation in human mesangial
520 cells through STAT3/NF-κB pathway. *Journal of Cellular Biochemistry 120,*
521 3467−3473. https://doi.org/10.1002/jcb.27621.
522 Ma, C., Xiao, H., & He, L. (2016). Surface-enhanced Raman scattering characterization
523 of monohydroxylated polymethoxyflavones: SERS behavior of monohydroxylated
524 polymethoxyflavones. *Journal of Raman Spectroscopy, 47*, 901−907.
525 https://doi.org/10.1002/jrs.4932.
526 Meier, B., & Spriano, D. (2010). Modern HPTLC–a perfect tool for quality control of
527 herbals and their preparations. *Journal of AOAC International, 93*, 1399−1409.
528 https://doi.org/10.1093/jaoac/93.5.1399.
529 Mikropoulou, E. V., Petrakis, E. A., Argyropoulou, A., Mitakou, S., Halabalaki, M.,
530 Skaltsounis, L. A. (2019). Quantification of bioactive lignans in sesame seeds using
531 HPTLC densitometry: Comparative evaluation by HPLC-PDA. *Food Chemistry,*
532 *288,* 1−7. https://doi.org/10.1016/j.foodchem.2019.02.109.
533 Oellig, C., Schunck, J., & Schwack, W. Determination of caffeine, theobromine and
534 theophylline in Mate beer and Mate soft drinks by high-performance thin-layer
535 chromatography. *Journal of Chromatography A, 1533*, 208−212.

https://doi.org/10.1016/j.chroma.2017.12.019.

Reguera, J., Langer, J., Jimenez, A. D., & Liz-Marzan, L. M. (2017). Anisotropic metal nanoparticles for surface enhanced Raman scattering. *Chemical Society Reviews, 46,* 3866−38856. https://doi.org/10.1039/c7cs00158d.

Sanchez-Cortes, S., & Garcia-Ramos, J. V. (2000). Adsorption and chemical modification of phenols on a silver surface. *Journal of Colloid and Interface Science, 231*, 98−106. https://doi.org/10.1006/jcis.2000.7101.

Sayuri, I. T., Suwa, R., Fukuzawa, Y., & Kawamitsu, Y. (2011). Polymethoxyflavones, synephrine and volatile constitution of peels of citrus fruit grown in Okinawa. *Japanese Society for Horticultural Science, 80*, 214−224. https://doi.org/10.2503/jjshs1.80.214.

Stremple, P. (2015). GC/MS analysis of polymethoxyflavones in citrus oils. *Journal of Separation Science, 21*, 587−591. https://doi.org/10.1002/(SICI)1521-4168(19981101)21:11<587::AID-JHRC587>3.0.CO;2-P.

Sundaram, R., Shanthi, P., & Sachdanandam, P. (2015). Tangeretin, a polymethoxylated flavone, modulates lipid homeostasis and decreases oxidative stress by inhibiting NF-κB activation and proinflammatory cytokines in cardiac tissue of streptozotocin-induced diabetic rats. *Journal of Functional Foods, 16*, 315−333. https://doi.org/10.1016/j.jff.2015.03.024.

Surichan, S., Arroo, R. R., Ruparelia, K., Tsatsakis, A. M., & Androutsopoulos, V. P. (2018). Nobiletin bioactivation in MDA-MB-468 breast cancer cells by

cytochrome P450 CYP1 enzymes. *Food & Chemical Toxicology, 113*, 228−235. https://doi.org/10.1016/j.fct.2018.01.047.

Wen, L., & Lu, X. (2016). Determination of chemical hazards in foods using surface-enhanced Raman spectroscopy coupled with advanced separation techniques. *Trends in Food Science & Technology, 54*, 103−113. https://doi.org/10.1016/j.tifs.2016.05.020.

Wojtanowski, K. K., Mroczek, T. (2018). Study of a complex secondary metabolites with potent anti-radical activity by two dimensional TLC/HPLC coupled to electrospray ionization time-of-flight mass spectrometry and bioautography. *Analytica Chimica Acta, 1029*, 104−115. https://doi.org/10.1016/j.aca.2018.03.066.

Zaffino, C., Bedini, G. D., Mazzola, G., Guglielmi, V., & Bruni, S. (2016). Online coupling of high-performance liquid chromatography with surface-enhanced Raman spectroscopy for the identification of historical dyes. *Journal of Raman Spectroscopy, 47*, 607−615. https://doi.org/10.1002/jrs.4867.

Zhang, H., Cui, J., Tian, G., Christina, D. C., Gao, W., Zhao, C., Li, G., Lian, Y., Xiao, H., & Zheng, J. (2019). Efficiency of four different dietary preparation methods in extracting functional compounds from dried tangerine peel. *Food Chemistry, 289*, 340−350. https://doi.org/10.1016/j.foodchem.2019.03.063.

Zhang, Y., Zhao, C., Tian, G., Lu, C., Li, Y., He, L., Xiao, H., & Zheng, J. (2018). Simultaneous characterization of chemical structures and bioactivities of citrus-derived components using SERS barcodes. *Food Chemistry, 240*, 743−750.

https://doi.org/10.1016/j.foodchem.2017.07.103.

Zhao, Z. H., S.; Hu, Y.; Yang, Y.; Jiao, B.; Fang, Q., & Zhou, Z. (2017). Fruit flavonoid variation between and within four cultivated citrus species evaluated by UPLC-PDA system. *Scientia Horticulturae, 224*, 93−101. https://doi.org/10.1016/j.scienta.2017.05.038.

Zheng, J., Bi, J., Johnson, D., Sun, Y., Song, M., Qiu, P., Dong, P., Decker, E., & Xiao, H. (2015). Analysis of 10 metabolites of polymethoxyflavones with high sensitivity by electrochemical detection in high-performance liquid chromatography. *Journal of Agricultural & Food Chemistry, 63*, 509−516. https://doi.org/10.1021/jf505545x.

Zheng, J., Fang, X., Cao, Y., Xiao, H., & He, L. (2013). Monitoring the chemical production of citrus-derived bioactive 5-demethylnobiletin using surface enhanced Raman spectroscopy. *Journal of Agricultural & Food Chemistry, 61*, 8079−8083. https://doi.org/10.1021/jf4027475.

Zheng, J., & He, L. (2014). Surface-enhanced Raman spectroscopy for the chemical analysis of food. *Comprehensive Reviews in Food Science & Food Safety, 13*, 317−328. https://doi.org/10.1111/1541-4337.12062.

Zheng, J., Song, M., Dong, P., Qiu, P., Guo, S., Zhong, Z., Li, S., Ho, C. T., & Xiao, H. (2013). Identification of novel bioactive metabolites of 5-demethylnobiletin in mice. *Molecular Nutrition & Food Research, 57*, 1999−2007. https://doi.org/10.1002/mnfr.201300211.

Zhu, Q., Chen, M., Han, L., Yuan, Y., & Lu, F. (2017). High efficiency screening of

599 nine lipid-lowering adulterants in herbal dietary supplements using thin layer
600 chromatography coupled with surface enhanced Raman spectroscopy. *Analytical*
601 *Methods, 9*, 1595−1603. https://doi.org/10.1039/C6AY03441A.

Figure captions

Fig. 1 (A) Chemical structures of 14 major citrus flavonoids; (B) TLC separation eluted with DCM: MT= 20: 1 containing 1% acetic acid; (C) TLC separation eluted with PE: AT= 6: 4; (D) 2D separation eluted with DCM: MT= 20: 1 containing 1% acetic acid and PE: AT= 6: 4 subsequently (R_f, retardation factor value; DCM, dichloride methylene; MT, methanol; PE, petroleum ether; AT, acetone; M, mixtures of compounds **1**-**14**).

Fig. 2 SERS analysis (1100-1800 cm^{-1}) after TLC separation of 14 citrus flavonoids. (A) The second-derivative SERS spectra; (B) PCA discrimination; (C) PLS analysis (compound **3** as an example).

Fig. 3 HPLC profiles (UV detector, 280 nm) of fresh orange juice sample (A), fresh orange peel sample (B), mice fecal sample fed with compound **7** (C) and mixture of 14 citrus flavonoid standards (D), and UV absorbance (190-500 nm) of 14 citrus flavonoids after HPLC separation (E).

Table 1 R_f value, visualization color and limit of detection of 14 citrus flavonoids on TLC plate (R_f, retardation factor value; DCM, dichloride methylene; MT, methanol; PE, petroleum ether; AT, acetone).

Table 2 Limit of quantitation, linearity, recovery rate and detection accuracy of TLC-SERS analysis for 14 citrus flavonoids.

Table 3 Determination of citrus flavonoids in three real samples using TLC-SERS and HPLC-UV methods (fresh orange juice sample, fresh orange peel sample, and mice fecal sample fed with compound **7**, respectively).

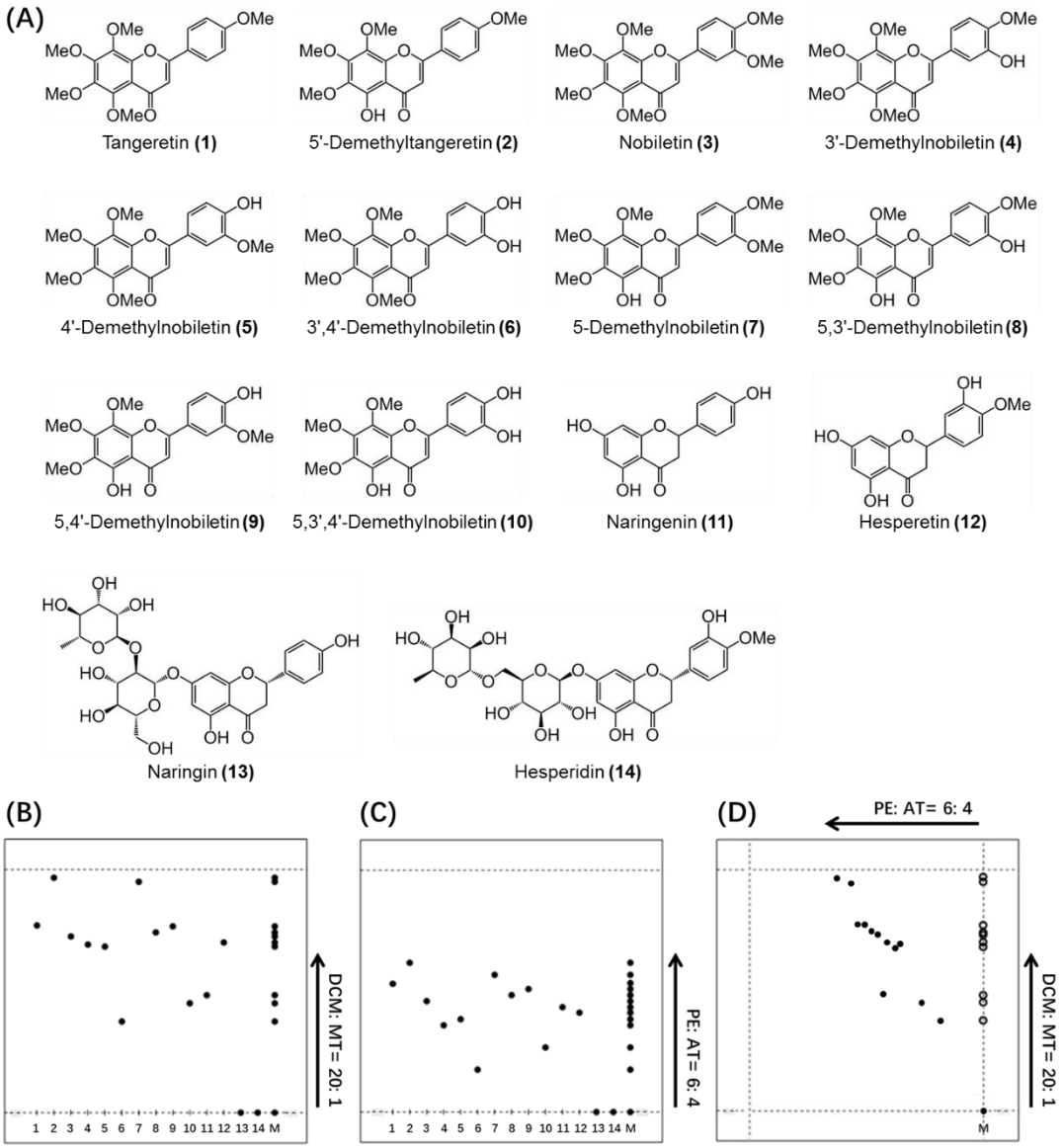

Fig. 1 (A) Chemical structures of 14 major citrus flavonoids; (B) TLC separation eluted with DCM: MT= 20: 1 containing 1% acetic acid; (C) TLC separation eluted with PE: AT= 6: 4; (D) 2D separation eluted with DCM: MT= 20: 1 containing 1% acetic acid and PE: AT= 6: 4 subsequently (R_f, retardation factor value; DCM, dichloride methylene; MT, methanol; PE, petroleum ether; AT, acetone; M, mixtures of compounds **1**-**14**).

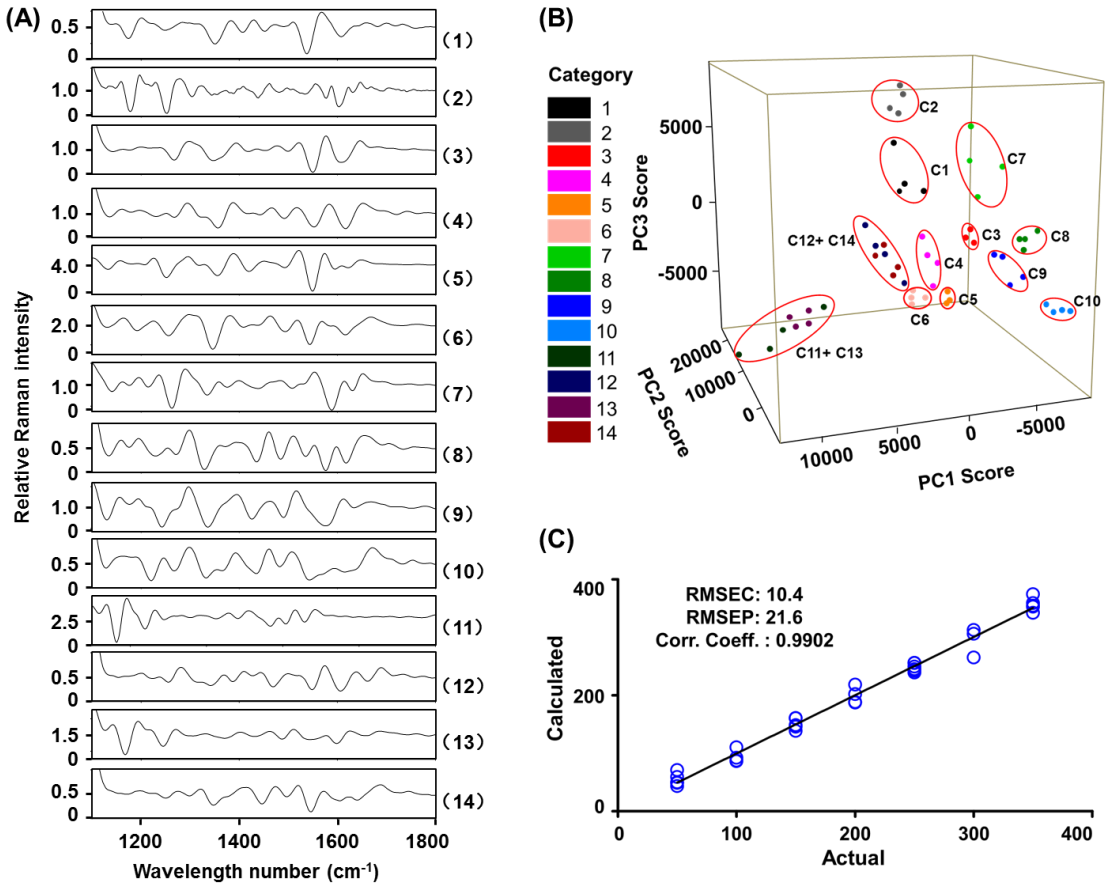

631

632 **Fig. 2** SERS analysis (1100-1800 cm^{-1}) after TLC separation of 14 citrus flavonoids.

633 (A) The second-derivative SERS spectra; (B) PCA discrimination; (C) PLS

634 analysis (compound **3** as an example).

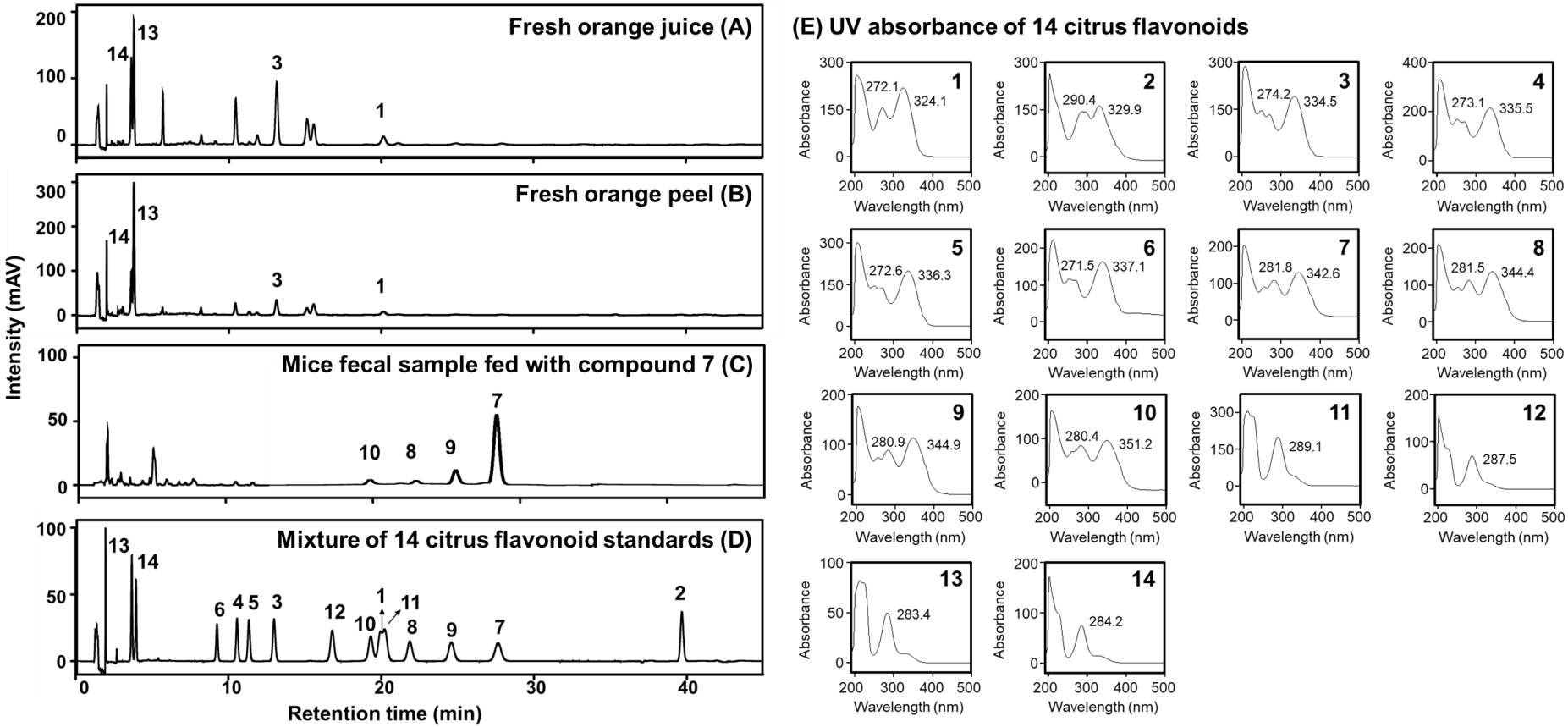

635 **Fig. 3** HPLC profiles (UV detector, 280 nm) of fresh orange juice sample (A), fresh orange peel sample (B), mice fecal sample fed with compound
636 **7** (C) and mixture of 14 citrus flavonoid standards (D), and UV absorbance (190-500 nm) of 14 citrus flavonoids after HPLC separation
637 (E).

Table 1 R_f value, visualization color and limit of detection of 14 citrus flavonoids on TLC plate (R_f, retardation factor value; DCM, dichloride methylene; MT, methanol; PE, petroleum ether; AT, acetone).

Compounds	R_f value		Visualization				Limit of detection (mM)			
			UV fluorescence		Staining		UV fluorescence		Staining	
	DCM: MT = 20: 1	PE: AT = 6: 4	254 nm	365 nm	Vanillin-H_2SO_4	$FeCl_3$	254 nm	365 nm	Vanillin-H_2SO_4	$FeCl_3$
1	0.77	0.53	Dark	Yellow	Yellow	-	0.5	0.5	0.5	-
2	0.97	0.62	Dark	Yellow	Yellow	Gray	1	1	5	5
3	0.73	0.46	Dark	Blue	Yellow	-	0.5	0.1	0.5	-
4	0.69	0.36	Dark	Blue	Yellow	Yellow	0.5	0.1	0.5	5
5	0.68	0.38	Dark	Blue	Yellow	Yellow	0.5	0.1	0.5	5
6	0.38	0.18	Dark	Blue	Yellow	Yellow	0.5	0.5	0.5	5
7	0.95	0.57	Dark	Yellow	Yellow	Gray	1	1	5	5
8	0.74	0.48	Dark	Yellow	Yellow	Gray	0.5	0.5	5	5
9	0.77	0.51	Dark	Yellow	Yellow	Gray	0.5	0.5	5	5
10	0.45	0.27	Dark	Yellow	Yellow	Gray	0.5	0.5	5	5
11	0.48	0.43	Dark	Dark	-	Brown	2.5	2.5	-	5
12	0.7	0.42	Dark	Dark	-	Brown	2.5	2.5	-	5
13	0	0	Dark	Blue	-	Brown	0.5	1	-	1
14	0	0	Dark	Blue	-	Brown	0.5	1	-	1

641 **Table 2** Limit of quantitation, linearity, recovery rate and detection accuracy of TLC-SERS analysis for 14 citrus flavonoids.

		Linearity				Recovery rate				Precision	
						50 μM		100 μM		50 μM	100 μM
Comp.	LOD (μM)	Conc. range (μM)	RMSEC	RMSEP	Correlation coefficient	Recovery rate	RSD (%)	Recovery rate	RSD (%)	RSD (%)	RSD (%)
1	16.7	50−200	14.3	31.2	0.9690	113.4	12.7	100.4	2.5	11.8	6.4
2	16.7	50−350	20.0	39.6	0.9859	107.2	15.4	112.5	7.9	7.6	8.9
3	16.7	50−350	10.4	21.6	0.9902	121.7	12.6	104.8	3.2	6.9	7.0
4	16.7	50−350	32.8	34.0	0.9546	107.7	3.9	96.5	5.7	6.6	7.2
5	10	30−200	5.5	19.6	0.9960	110.9	14.7	105.3	15.8	1.5	6.8
6	10	30−300	19.9	17.9	0.9821	106.1	20.8	113.2	1.8	6.0	4.3
7	10	30−350	19.4	25.8	0.9877	102.9	19.9	97.4	15.0	5.7	9.2
8	16.7	50−200	17.4	36.6	0.9545	91.5	8.0	98.5	4.3	6.5	9.6
9	10	30−150	11.6	27.6	0.9544	114.8	1.4	94.2	13.6	4.6	6.6
10	10	30−300	16.6	26.6	0.9879	111.0	17.6	117.3	8.3	8.9	5.0
11	10	30−300	9.3	12.9	0.9962	110.5	18.9	95.6	7.3	2.5	5.5
12	10	30−250	9.8	18.8	0.9940	118.7	12.1	99.2	15.4	9.2	5.8
13	10	30−300	17.6	18.8	0.9862	102.0	9.6	102.8	5.2	6.7	6.5
14	10	30−300	17.7	13.1	0.9851	116.6	18.3	104.8	7.9	8.6	9.0

642

643 **Table 3** Determination of citrus flavonoids in three real samples using TLC-SERS and HPLC-UV methods (fresh orange juice sample, fresh orange peel sample,
644 and mice fecal sample fed with compound **7**, respectively).

Comp.	Sample 1 (μg/mL)				Sample 2 (μg/g)				Sample 3 (ng/g)				Time (min)		
	1	**3**	**13**	**14**	**1**	**3**	**13**	**14**	**7**	**8**	**9**	**10**	**Separation**	**Detection**	**Total**
TLC-SERS	3.9 ± 0.1	46.0 ± 2.7	87.8 ± 7.7	164.9 ± 12.2	43.2 ± 3.1	212.5 ± 6.4	467.1 ± 27.3	986.5 ± 94.8	34.6 ± 0.6	3.7 ± 0.3	11.1 ± 0.5	29.3 ± 0.7	8	2	10
HPLC-UV	3.6 ± 0.1	43.7 ± 1.3	85.7 ± 3.1	222.7 ± 5.6	40.0 ± 2.6	259.6 ± 4.1	427.9 ± 18.1	1217.9 ± 61.4	44.8 ± 1.4	3.0 ± 0.1	10.4 ± 0.1	36.4 ± 0.2	45	0	45
Deviation (%)	7.1	5.3	2.4	25.9	8.2	18.1	9.2	19.0	22.8	20.0	6.0	19.7	Reduced 77.8%		

645